Nanoscale

Accepted Manuscript

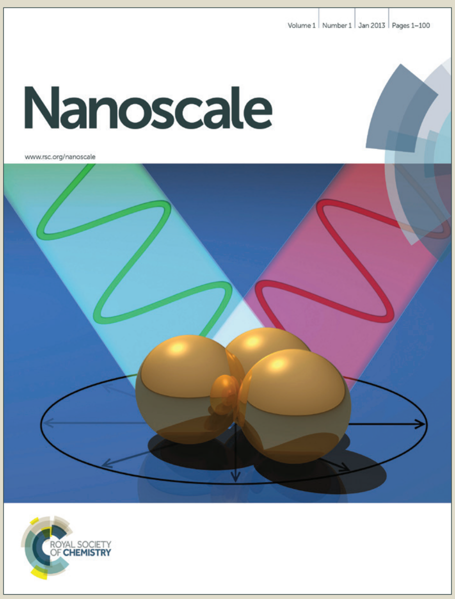

Nanoscale Guidelines to Referees

Nanoscale (**www.rsc.org/nanoscale**) is a community-spanning journal publishing very high quality, high impact research across nanoscience and nanotechnology.

Nanoscale's latest Impact Factor is 6.23

We aspire to even higher values in future years

The Editors stress very high standards for acceptance in *Nanoscale*. Articles must report extremely novel, very high quality, reproducible new work of broad general interest.

As a referee, the Editors-in-Chief strongly encourage you to recommend only the best work for publication in *Nanoscale*. Since launch in late 2009, *Nanoscale* has quickly become a leading journal. The Editors aspire for the journal to publish truly world-class research.

Routine, limited novelty or incremental work – even if competently researched and reported - should **not** be recommended for publication. ***Nanoscale* demands high novelty and high impact**.

We strongly discourage fragmentation of work into several short publications. Unnecessary fragmentation is a valid reason for rejection.

Thank you very much for your assistance in evaluating this manuscript, which is greatly appreciated.

With our best wishes,

Chunli Bai, Jie Liu, Wei Lu, Francesco Stellacci, Serena Corr, Dirk Guldi, Xingyu Jiang, Rongchao Jin, Shouheng Sun, Jianfang Wang, Xiao Cheng Zeng (Editors)

General Guidance (For further details, see RSC Publishing's Refereeing Procedure and Policy**)**

Referees have the responsibility to treat the manuscript as confidential. Please be aware of our **Ethical Guidelines** which contain full information on the responsibilities of referees and authors.

When preparing your report, please:
• Comment on the originality, importance, impact and scientific reliability of the work;
• State clearly whether you would like to see the paper accepted or rejected and give detailed comments (**with references**) that will both help the Editor to make a decision on the paper and the authors to improve it;

Please inform the Editor if:
• There is a conflict of interest;
• There is a significant part of the work which you are not able to referee with confidence;
• If the work, or a significant part of the work, has previously been published, including online publication, or if the work represents part of an unduly fragmented investigation.

When submitting your report, please:
• Provide your report rapidly and within the specified deadline, or inform the Editor immediately if you cannot do so. We welcome suggestions of alternative referees.

If you have any questions about reviewing this manuscript, please contact the Editorial Office at **nanoscale@rsc.org**

Dear Prof. Jie Liu

Thank you for sending us the reviewer's comments on the manuscript NR-ART-02-2014-001107 "A Facile Route to Monodisperse MPd (M = Co or Cu) Alloy Nanoparticles and Their Catalysis for Electrooxidation of Formic Acid".

We thank to the reviewers for their kind comments and recommendations. Although the reviewers did not indicate any revisions, we have checked the manuscript and SI part one more time carefully. Moreover, we added a "Table of Contents" entry for this submission at the end of the main text.

We believe that the manuscript is now ready for publication in Nanoscale. Thank you for your consideration.

Journal Name

Nanoscale

Dynamic Article Links ►

Cite this: DOI: 10.1039/c0xx00000x

www.rsc.org/xxxxxx

ARTICLE TYPE

A Facile Route to Monodisperse MPd (M = Co or Cu) Alloy Nanoparticles and Their Catalysis for Electrooxidation of Formic Acid

Sally Fae Ho,[a] Adriana Mendoza-Garcia,[a] Shaojun Guo,[a] Kai He,[b] Dong Su,[b] Sheng Liu,[a] Önder Metin,[a,c] and Shouheng Sun[a,*]

Received (in XXX, XXX) Xth XXXXXXXXX 20XX, Accepted Xth XXXXXXXXX 20XX

MPd (M = Co, or Cu) nanoparticles (NPs) were synthesized by borane-amine reduction of metal acetylacetonates. The size of the MPd NPs was controlled at 3.5 nm and their compositions were tuned by the molar ratios of the metal precursors. These MPd NPs were active catalyst for electrochemical oxidation of formic acid and the $Cu_{30}Pd_{70}$ NPs showed the highest mass activity at 1192.9A/g_{Pd}, much higher than 552.6 A/g_{Pd} obtained from the 3.5 nm Pd NPs. Our synthesis provides a facile route to MPd NPs, allowing further investigations of MPd NP catalysts for electrochemical oxidation and many other chemical reactions.

Synthesis of nanoparticles (NPs) of palladium (Pd) and its alloys with first-row transition metals has attracted much attention due to the important catalytic roles these NPs play in a variety of chemical reactions,[1] including electrochemical oxidation of formic acid (FA)[2]. Conventionally, the FA oxidation reaction (FAOR) is catalyzed by platinum (Pt) catalysts and is used to couple with the oxygen reduction reaction in direct FA fuel cells to convert chemical energy stored in FA into electric energy. However, Pt catalysts developed for the FAOR are prone to CO poisoning due to the formation of CO from FA dehydration reactions and strong Pt-CO binding.[3] In the efforts to develop an advanced catalyst with high CO-tolerance, nanostructured Pd materials have come to light.[4] Studies show that accumulation of CO on the surface of Pd is very slow,[5] and Pd's resistivity to surface deactivation can be further enhanced when an early transition metal (M) is present adjacent to Pd, making MPd NPs an important class of catalysts for the FAOR.[6] Therefore, it is important to prepare monodisperse MPd alloy NPs with controlled sizes and compositions so that their catalysis for FAOR can be tuned and optimized.

Here we report a facile and generalized synthesis of monodisperse MPd NPs (M = Co or Cu). Previously, MPd NPs were prepared by impregnation,[7a,b,] sputtering,[7c] acidic dealloying[7d], and electrodeposition [7e] methods with limited size and morphology control. We have recently showed that monodisperse CoPd and CuPd alloy NPs could be prepared in the presence of oleylamine (OAm) and trioctylphosphine (TOP).[8] However, the presence of multiple surfactants, especially TOP, around the MPd NPs makes it difficult to activate MPd NPs for catalytic studies. Different from our previous synthetic protocols, the current method applies a simple organic phase co-reduction of metal acetylacetonate, $M(acac)_2$, and $Pd(acac)_2$ by borane *t*-butylamine (BBA) in OAm and 1-octadecene (ODE). In this protocol, BBA serves as a mild reducing agent, OAm acts as the surfactant and ODE is used as solvent. In the current reaction condition, MPd NPs are synthesized with an average size of 3.5 nm. This size controlled synthesis made it possible to study M-dependent catalysis for FAOR. Our studies showed that CuPd NPs were more efficient catalyst than the CoPd NPs. For $Cu_{30}Pd_{70}$ NPs, their mass activity reaches 1192.9 A/g_{Pd}. To our knowledge, this is the highest mass activity value ever reported for a Pd-based NP catalyst.[8a, 9]

Monodisperse MPd NPs were synthesized by injecting the OAm solution of $M(acac)_2$ and $Pd(acac)_2$ into the OAm/ODE solution of BBA. The injection induced a burst co-nucleation of M and Pd, facilitating the formation of MPd alloy NPs with controlled size and composition. For example, to synthesize $Co_{30}Pd_{70}$ NPs, 3 mL OAm solution consisting of 0.3 mmol of $Pd(acac)_2$ and 0.3 mmol of $Co(acac)_2$ was injected into the OAm/ODE (3 mL OAm and 7 mL ODE) solution of BBA (2.3 mmol) at 100°C under vigorous magnetic stirring. The reaction was allowed to proceed for 1 h and then cooled down to room temperature before acetone/ethanol was added to precipitate/wash CoPd NPs. The CoPd NPs were redispersed in hexane for further use.

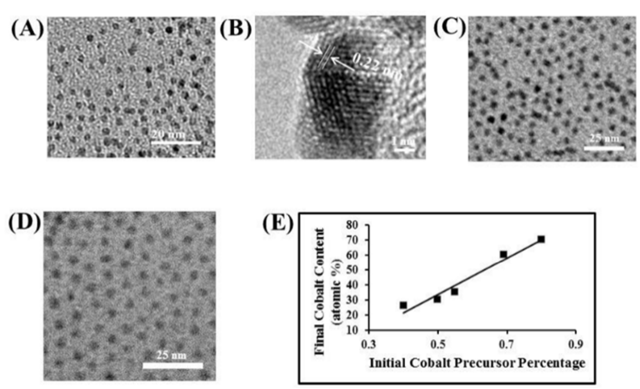

Fig.1 (A) TEM image of $Co_{30}Pd_{70}$, (B) HR-TEM image of $Co_{30}Pd_{70}$, (C) TEM image of $Co_{45}Pd_{55}$, and (D) TEM image of $Co_{70}Pd_{30}$ NPs. (E) Relationship between initial cobalt molar ratio and final cobalt content in NPs.

Fig. 1A is a representative transmission electron microscopy (TEM) image of the as synthesized $Co_{30}Pd_{70}$ NPs and **Fig. 1B** shows are the high resolution TEM (HRTEM) of a single CoPd NP. Their size is measured to be 3.35 ± 0.32 nm. The CoPd NPs have a measured interfringe spacing of 0.22 nm, close to the interplanar distance of Pd (111) planes (0.223 nm). The composition of these NPs can be controlled by tuning metal precursor ratios. For example, 0.45 mmol of $Co(acac)_2$ and 0.11 mmol of $Pd(acac)_2$ yielded $Co_{70}Pd_{30}$ (**Fig. 1C**) and 0.25 mmol of $Co(acac)_2$ and 0.11 mmol $Pd(acac)_2$ yields $Co_{55}Pd_{45}$. **Fig. 1E** shows a linear correlation between the initial amount of Co precursor and the final atomic percentage of Co in the NPs, indicating that Co is readily incorporated into the NP structure.

The method used for the synthesis of CoPd NPs could be readily extended to prepare Pd NPs. To synthesize 3.5 nm Pd NPs, 0.25 mmol $Pd(acac)_2$ was first dissolved in 3 mL of OAm, and subsequently injected into a mixture of 2.3 mmol of BBA, 3 mL of OAm and 7 mL ODE at 100°C. **Fig. S1** shows the Pd NPs of 3.55 ± 0.43 nm in diameter.

To prepare the CuPd NPs, we found that morpholine borane (MB), instead of BBA, was better used to control the Cu/Pd composition at a lower injection temperature of 80°C. Our tests indicated that BBA reduced $Pd(acac)_2$ too quickly compared to $Cu(acac)_2$, which could lead to separate nucleation events and the formation of a mixture of Pd and CuPd. A milder reducing agent, such as MB,[10] and lower injection temperature could solve this problem and produced monodisperse CuPd NPs with controlled sizes and compositions. $Cu_{30}Pd_{70}$ NPs were prepared by first dissolving 0.15 mmol of $Cu(acac)_2$ and 0.35 mmol of $Pd(acac)_2$ into 3 mL of OAm. This solution was then injected into a mixture of MB (1.5 mmol), 3 mL OAm and 7 mL ODE at 80°C; the reaction mixture was subsequently raised to 100°C and kept at that temperature for 1 h. In the current reaction condition, Cu-rich alloys, $Cu_{75}Pd_{25}$ or $Cu_{62}Pd_{38}$ NPs could be produced by MB-reduction of 0.35 mmol $Cu(acac)_2$ and 0.1 mmol $Pd(acac)_2$ or 0.3 mmol $Cu(acac)_2$ and 0.3 mmol $Pd(acac)_2$ respectively.

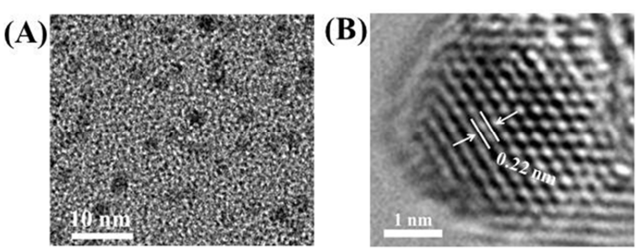

Fig. 2 (A) TEM image of $Cu_{30}Pd_{70}$ NPs and (B) HRTEM image of a single $Cu_{70}Pd_{30}$ NP.

Fig. 2A is a representative TEM image of the $Cu_{30}Pd_{70}$ NPs. They are measured to be 3.38 ± 0.33 nm in diameter. The HRTEM image of a single CuPd NP (**Fig. 2B)** shows an interfringe distance of 0.22 nm. This values is close to the (111) interplanar spacing of *fcc*-Pd (0.223 nm) and *fcc*-Cu (0.21 nm). We further characterized the NP structure by XRD. **Figure 3** shows the XRD patterns of the CuPd, as well as Pd and CoPd NPs. The (111) peaks are broad and shift to slight higher angel from Pd (2□ = 39.76°), CuPd (2□ = 39.98°) to CoPd (2□ = 40.1°). Using Scherrer's equation, we estimated the crystal domain sizes of the CuPd and CoPd NPs to be 1.1 and 2.1 nm, respectively, which are all smaller than what are measured from TEM analyses. These results confirm the solid solution and polycrystalline nature within MPd NPs.

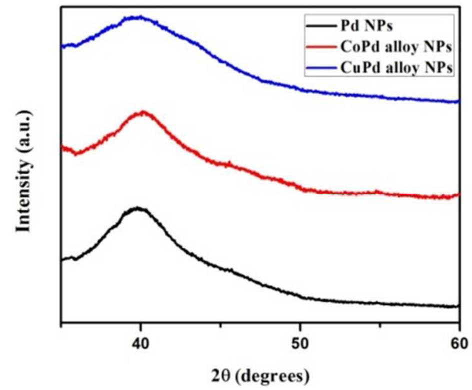

Fig. 3 XRD patterns of Pd and MPd NPs

The injection of the metallic precursors into the reducing agent solution at a properly controlled temperature is a key for the alloy formation as it ensures the simultaneous reduction of the precursors and co-nucleation/growth of MPd alloys. We can even alter the NP size and composition by simply changing the injection and growth temperature. For example, 0.3 mmol of $Co(acac)_2$ and 0.3 mmol of $Pd(acac)_2$ injected and kept at 75 °C leads to 3.08 ± 0.38 nm $Co_{25}Pd_{75}$ NPs. At 125 °C, 4.11 ± 0.34 nm $Co_{37}Pd_{63}$ NPs are formed (**Fig. S2)**. Our synthesis differs from the previous approach to CoPd NPs,[8a] in which high temperatures (> 265 °C) were required to facilitate the decomposition and reduction of the metal precursors in the presence of OAm and TOP. TOP was the key in the previous synthesis to achieve NP composition and morphology control on CoPd alloy NPs. However, TOP is tightly associated with the NPs due to the strong π-backbonding between Pd and P, making it difficult to remove TOP to activate the NPs for catalytic studies. In our new protocol, BBA or MB is used as a reducing agent and OAm as the surfactant. NPs stabilized by OAm are more readily activated due to the weaker $-NH_2$-Pd binding.

Pd NPs have been shown to be active catalysts for the formic acid oxidation reaction (FAOR).[6,11] This is because Pd facilitates oxidation *via* a direct 2 electron oxidation pathway (Eq. 1) in comparison to an indirect pathway seen on Pt catalysts (Eqs. 2-1 and 2-2), which requires higher overpotentials for complete oxidation.[6,11]

$$HCOOH \rightarrow CO_2 + 2H^+ + 2e^- \qquad \text{(Eq. 1)}$$
$$HCOOH \rightarrow CO_{ad} + H_2O \qquad \text{(Eq. 2-1)}$$
$$CO_{ad} + H_2O \rightarrow CO_2 + 2H^+ + 2e^- \qquad \text{(Eq. 2-2)}$$

To oxidize FA into carbon dioxide and hydrogen, the O-H and C-H bonds must be broken. The O-H bond is readily broken by Pd in the entire potential range, whereas Pt can break the C-O/C-H bond at lower overpotentials but requires high overpotentials to break the O-H bond.[6,12] FAOR on Pt surfaces proceeds *via* a dehydration pathway; the CO product ultimately adsorbs onto the surface, hindering active sites and deactivating the catalyst. Pd promotes the dehydrogenation pathway,[5] making it a promising candidate as an anode catalyst for FAOR. Alloying Pd with different first-row transition metals changes its electronic structure and can further enhance its FAOR activity.[6d,e]

To study MPd NPs for FAOR, we deposited the MPd NPs on Ketjen carbon support by mixing and sonicating the mixture at a 1:2 NP:C weight ratio in 50 mL of hexane/acetone (v/v 1/1). The catalyst, denoted as C-MPd, was separated by centrifugation and washed with hexane twice. To activate C-MPd for the FAOR, we annealed it in air overnight at 150°C. From our preliminary FAOR testing on different C-CoPd NPs, we found that the $Co_{30}Pd_{70}$ exhibited the highest activity. Therefore, we chose the $M_{30}Pd_{70}$ for an in-depth electrochemical study.

The TEM image of the annealed and activated C-$Co_{30}Pd_{70}$ (**Fig. S3**) showed that the NPs had no visible morphology and size change during the treatment. XRD of the annealed C-$Co_{30}Pd_{70}$ indicated no obvious oxide formation. The C-NP catalyst was suspended in a mixture of D. I. water, 2-propanol, 5% Nafion at the volume ratio of 4/1/0.05 under sonication to form a 4 mg/mL ink. 5 µL of this ink, containing 0.02 mg of MPd, was dropped onto the surface of the glassy carbon (GC) working electrode and dried under ambient conditions.

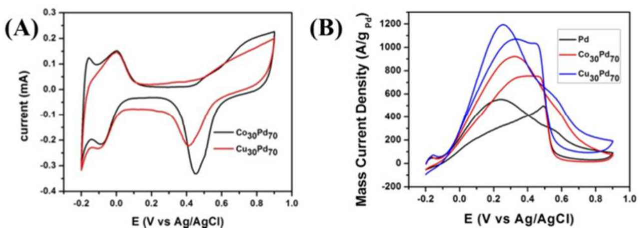

Fig. 4. (**A**) CVs of $M_{30}Pd_{70}$ NPs at 25 °C in N_2 saturated $HClO_4$ (scan rate = 50 mV/s). (**B**) CV curves of the three different NP catalysts at 25°C in N_2 saturated 0.1 M $HClO_4$ and 0.1 M HCOOH. (scan rate = 50 mV/s).

Figure 4A is the cyclic voltammetric (CV) scans of two different MPd NPs in N_2 saturated $HClO_4$ solution. The peak in the -0.2 to 0.1 V range is attributed to proton reduction/hydrogen adsorption (from 0.1 to -0.2 V) and hydrogen oxidation/desorption (from -0.2 to 0.1 V) on the NP surface. The catalyst is oxidized at potentials higher than 0.5 V and the oxidized species are reduced in the negative scan direction in the 0.6-0.3 V range. Because all the NPs have similar Pd content, the observed current intensity is largely influenced by the M. Because of the incorporation of M with Pd, we expect the reduction peaks of both CoPd and CuPd NPs to shift from Pd (0.44 V). The reduction peak from the CoPd occurs at 0.45 V while that from the CuPd appears at 0.4 V. The proximity between the CoPd and Pd seems to indicate that the surface of the CoPd is predominated by Pd. As comparison, the observed reduction peak at 0.4 V for the CuPd NPs infers that both Cu and Pd appear on the CuPd surface. Our controlled etching experiments also showed that Co in CoPd was more easily etched than Cu in CuPd.

The catalytic activity of the C-MPd and C-Pd on FAOR were evaluated in 0.1 M $HClO_4$ + 0.1 M HCOOH. The oxidation current obtained from FAOR in the -0.2 to 0.9 V region were normalized against the Pd weight for each catalyst as measured by ICP and shown in **Fig. 4B**. In the positive scan, FA is oxidized and the current is M/Pd composition dependent with CuPd showing the highest current value. At more positive potentials, the alloy is oxidized, leading to the decrease in activity and the drop of the current. In the reverse cathodic scan, the oxidized NP surface is reduced and FA is instantly oxidized as indicated by the sudden increase in the current. From **Fig. 4B**, we can see that the MPd catalysts show exceptional enhancement in mass activity compared to the monometallic Pd. The C-Pd catalyst has a peak potential at 0.239 V with a corresponding mass activity of 552.6 A/g_{Pd}. This value is higher than what we observed in FAOR catalyzed by 7 nm TOP stabilized Pd NPs. Comparing with different C-MPd catalysts, we see that there is a 10 mV and 80 mV positive shift in the peak oxidation potential of the C-$Cu_{30}Pd_{70}$ and C-$Co_{30}Pd_{70}$ catalysts, accompanied with a significant increase in current density. Among the MPd catalysts evaluated, the $Cu_{30}Pd_{70}$ catalyst exhibits the highest current density of 1192.9A/g_{Pd} at 0.254 V *vs* Ag/AgCl. In the negative scan, we observe a similar trend between Pd and the $M_{30}Pd_{70}$ catalysts; once again the MPd catalysts exhibit greater mass activity than Pd with CuPd showing the highest activity.

From the data presented, the M in MPd enhances the NP catalysis for FAOR. All the catalysts were treated equally and have similar compositions. ICP analysis after the reaction showed $Co_{30}Pd_{70}$ and $Cu_{30}Pd_{70}$ had final compositions of Co_5Pd_{95} and Cu_7Pd_{93}. Since the CoPd and CuPd catalysts have similar final composition after the FAOR tests, we can conclude that the difference in activity must be attributed to the electronic effect of M on the MPd alloy structure. The presence of less electropositive Cu in CuPd must be better optimized for the dehydrogenation reaction, promoting more favorably HCOOH adsorption and dehydrogenation on Pd than Co does on Pd.

In conclusion, we have presented a facile approach to monodisperse MPd (M = Co, or Cu) NPs *via* borane-amine reduction of metal acetylacetonates. The NP size was controlled at 3.5 nm and their compositions were easily tuned by altering the metal precursor ratios. The polycrystalline MPd NPs can be readily activated for catalytic FAOR with $M_{30}Pd_{70}$ NPs displaying higher activity than Pd NPs and $Cu_{30}Pd_{70}$ NPs exhibiting the mass activity of 1192.9 A/g_{Pd}. This report provides experimental support of the synergistic effect between the constituent metals in the MPd system on their role in catalytic activity enhancement. These MPd NPs should not be limited to catalyze just FAOR, but many other chemical reactions as well.

Acknowledgements

This work was supported by the U.S. Army Research Laboratory and the U.S. Army Research Office under the Multi University Research Initiative MURI grant number W911NF-11-1-0353 on "Stress-Controlled Catalysis via Engineered Nanostructures".

Notes and references

[a] *Department of Chemistry Brown University, Providence, Rhode Island, 02912, United States; *E-mail: ssun@brown.edu*
[b] *Brookhaven National Laboratory, Center for Functional Nanomaterials, Upton, NY 11973-5000, USA*
[c] *Department of Chemistry, Faculty of Science, Atatürk University, 25240 Erzurum, Turkey*

† Electronic Supplementary Information (ESI) available: Detailed synthetic and electrochemical analysis procedures, and XRD of the NPs. See DOI: 10.1039/b000000x/

1 (a) H. Li, L. Han, J. Cooper-White, and I. Kim, *Green Chem.*, 2012, **14**, 586. (b) A. J. Hickman and M. S. Sanford, *Nature*, 2012, **484**, 177. (c) Y. Sun, P. Zhu, Q. Xu and M. Shi, *RSC Advcances*, 2013, **3**, 3153. (d) Ö. Metin, S. Duman, M. Dinc, and S. Özkar, *J. Phys. Chem. C*, 2011, **115**, 10736. (e) S. Zhang, Ö. Metin, D. Su, and S. Sun, *Angew. Chem Int. Ed.* 2013, **52**, 3681. (f) Ö. Metin, E. Kayhan, S. Özkar and J.J. Schneider, *Int. J. Hydrogen Energy* 2012, **37**, 8161.

2 (a) C. Xu, Y. Liu, J. Wang, H. Geng, and H. Qiu, *J. Power Sources*, 2012, **199**, 124-131. (b) L. Zhang, J. Zhang, Z. Jiang, S. Xie, M. Jin, X. Han, Q. Kuang, Z. Xie and L. Zheng, *J. Mater. Chem.*, 2011, **21**, 9620. (c) Y. Lu and W. Chen, *ACS Catal.* 2011, **2**, 84-90.

3 (a) S. G. Sun, J. Claviler, A. Bewick. *J. Electroanal. Chem*. 1988, **240**, 147-159. (b) M. Fayette, J. Nutariya, N. Vasiljevic, N. Dimitrov, *ACS Catal*. 2013, **3**, 1700-1718.

4 (a) V. Mazumder and S. Sun, *J. Am. Chem. Soc.*, 2009, **131**, 4588; (b) X-M. Wang, and Y-X. Xia. *Electrochim. Acta.*, 2009, **54**, 7525; (c) H. Huang and X. Wang. *J. Mater. Chem.*, 2012**, 22**, 22533; (d) S. Wang and A. Manthiram. *Electrochim. Acta.*, 2013, **88**, 565; (e) Z. Bai, H. Yan, F. Wang, L. Yang and K. Jiang; *Ionics*, 2013 , **19**, 543.

5 H. Miyake, T. Okada, G. Samjekse, and M. Osawa. *Phys. Chem. Chem. Phys*. 2008, **10**, 3662-3669.

6 S. Uhm, H. J. Lee and J. Lee, *Phys. Chem. Chem. Phys*. 2009, **11**, 9326.

7 (a) J. P. Singh, X.G. Zhang, H. Li, A. Singh and R. N. Singh, *J. Electrochem. Sci.*, 2008, **3**, 416; (b) G. Ramos-Sanchez, M. M. Bruno, Y. R. J. Thomas, H. R. Corti, and O. Solorza-Feria, *Int. J. Hydrogen Energ*. 2012, **37**, 31; (c) O. Savadogo, K. Lee, K. Oishi, S. Mitsushima, N. Kamiya, and K. I. Ota, *Electochem. Commun.* 2004, **6**, 105; (d) W. Wang, S. Ji, H. Wang, and R. Wang, *Fuel Cells*, 2012, **12**, 1129; (e) C. Du, M. Chen, W. Wang, G. Yin and P. Shi, *Electrochem. Commun.*, 2010, **12**. 843.

8 (a) V. Mazumder, M. Chi, M. Mankin, Y. Liu, Ö. Metin, D. Sun, K. More, and S. Sun, *Nano Lett.* 2012, **12**, 1102. (b) D. Sun, V. Mazumder, Ö. Metin, S. Sun, *ACS Nano*, 2011, **5**, 6458-6464. (c) D. Sun, V. Mazumder, Ö .Metin and S. Sun, *ACS Catal*. 2012, **2**, 1290.

9 (a) W. Wang, S. Ji, H. Wang, and R. Wang, *Fuel Cells*, 2012, **12**, 1129; (b) C. Du, M. Chen, W. Wang, G. Yin and P. Shi, *Electrochem. Commun.*, 2010, **12**. 843. (c) C. Xu, Y. Liu, J. Wang, H. Geng, and H. Qiu. *J. Power Sources,* 2012**, 199**, 124; (d) R. Li, H. Hao, W-B. Cai, T. Huang and A. Yu. *Electrochem. Commun.* 2010, **12**, 901.

10 N. Zheng , J. Fan and G. D. Stucky, *J. Am. Chem. Soc.*, 2006, **128**, 6550–6551.

11 R. Larsen, S. Ha, J. Zakzeksi and R. I. Masel, *J. Power Sources*, 2006, **157**, 78.

12 X. Yu, and P. Pickup, *J. Power Sources*, 2008, **182**, 124.

Journal Name

Cite this: DOI: 10.1039/c0xx00000x

www.rsc.org/xxxxxx

ARTICLE TYPE

Table of Contents Entry

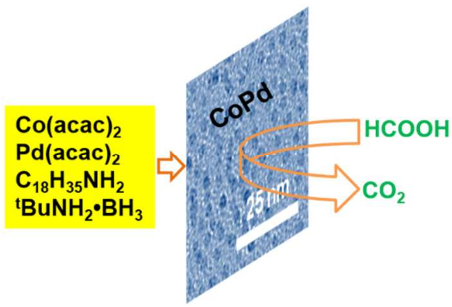

MPd (M: Co, Cu) nanoparticles were synthesized by borane-amine reduction of metal acetylacetonates and showed high catalytic performance in formic acid oxidation.

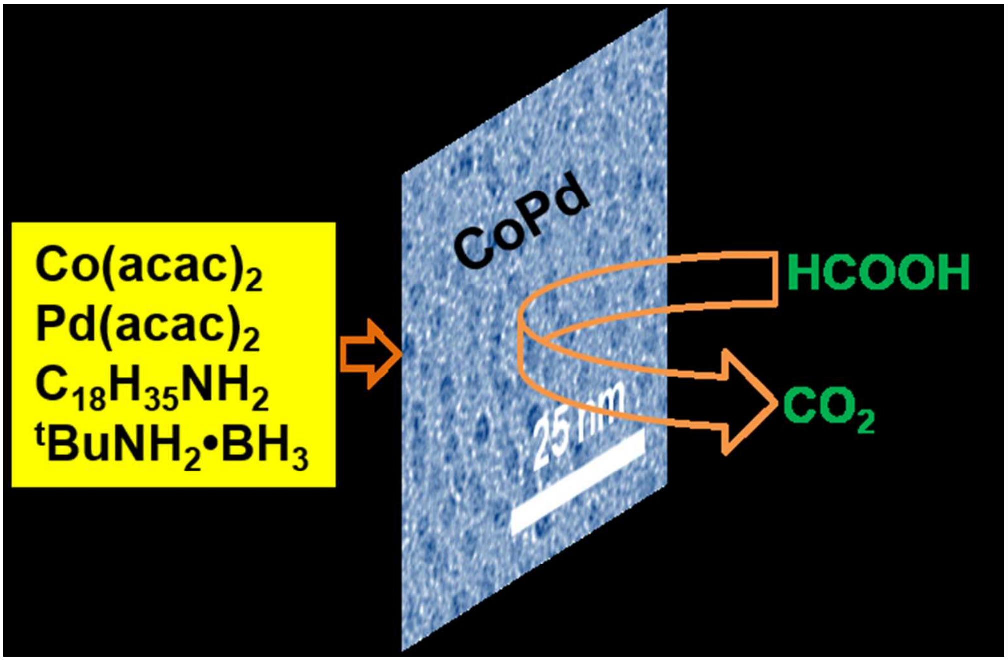

112x73mm (150 x 150 DPI)

Electronic Supplementary Information

A Facile Route to Monodisperse MPd (M = Co or Cu) Alloy Nanoparticles and Their Catalysis for Electrooxidation of Formic Acid

Sally Fae Ho,[a] Adriana Mendoza-Garcia,[a] Shaojun Guo,[a] Kai He,[b] Dong Su,[b] Sheng Liu,[a] Önder Metin,[a,c] and Shouheng Sun[a,*]

[a]Department of Chemistry, Brown University, Providence, RI 02912

[b]Brookhaven National Laboratory, Center for Functional Nanomaterials, Upton, NY 11973-5000, USA

[c]Department of Chemistry, Faculty of Science, Atatürk University, 25240 Erzurum, Turkey

[*]To whom correspondence should be addressed. E-mail: ssun@brown.edu

Experimental Section

The synthesis was carried out using standard airless procedures and commercially available reagents. All reagents were used as received. 1-Octadecene (ODE), oleylamine (OAm) (> 70%), morpholine borane (MB) (95%), borane *tert*-butylamine (BBA), palladium acetylacetonate ($Pd(acac)_2$, 99%), copper acetylacetonate ($Cu(acac)_2$), cobalt acetylacetonate ($Co(acac)_2$, > 97%), carbon monoxide (≥ 99%) and Nafion 117 were purchased from Sigma Aldrich. Nickel (II) acetate tetrahydrate ($NiAc_2{\bullet}4H_2O$, 98%) was obtained from Strem chemicals. Ketjen Black ($800m^2/g$) was obtained from Tanaka Precious Metals. ACS Grade formic acid (98%) was purchased from EMD.

Synthesis of 3.5 nm $Co_{30}Pd_{70}$ NPs

0.2 g of BBA was mixed with 3 mL of OAm and 7 mL of ODE and heated to 100°C. Separately, 0.3 mmol $Co(acac)_2$ and 0.3 mmol $Pd(acac)_2$ were dissolved in 3 mL of OAm at room temperature and injected into the 100 °C solution. The reaction was maintained at 100°C for 1 h and subsequently cooled to room temperature. The NPs were separated from the solution by adding acetone and centrifugation. The NPs were dispersed in hexane and precipitated by ethanol and centrifugation. The purified NPs were then dispersed in hexane for further use.

Composition Control of CoPd NPs.

In similar conditions described in the synthesis of CoPd NPs, changing the composition of the starting metal precursor ratio leads to different composition CoPd NPs. For instance, reaction of 0.45 mmol or 0.25 mmol of $Co(acac)_2$ with 0.11 mmol $Pd(acac)_2$ yielded $Co_{70}Pd_{30}$ or $Co_{55}Pd_{45}$ NPs respectively.

Synthesis of $Cu_{30}Pd_{70}$ NPs

0.2 g of MB was mixed with 3 mL of OAm and 7 mL of ODE and heated to 80°C. Separately, 0.15 mmol $Cu(acac)_2$ and 0.35 mmol $Pd(acac)_2$ were dissolved in 3 mL of OAm at room temperature and injected into the 80 °C mixture. The reaction was raised to 100°C for 1 h and subsequently cooled to room temperature. The NPs were separated from the solution with a similar process described in the synthesis of CoPd NPs. $Cu_{75}Pd_{25}$ or $Cu_{62}Pd_{38}$ NPs could be produced by changing the starting Cu:Pd molar precursor ratios to 0.35:0.1 or 0.3:0.3, respectively.

Synthesis of 3.5 nm Pd NPs

These NPs were synthesized in similar conditions as the CoPd NPs, using 0.25 mmol of $Pd(acac)_2$.

NP Characterization

Samples for transmission electron microscopy (TEM) analysis were prepared by depositing a single drop of the diluted NP dispersion in hexane on amorphous carbon coated copper grids. Images were obtained on a Philips CM20 at 200 kV. High resolution TEM (HRTEM) images were obtained on a JEOL 2100F with an accelerating voltage of 200 kV. XRD patterns were recorded on a Bruker D8 Discover (Cu Kα). Inductively coupled plasma (ICP) elemental analysis measurements were carried out on a JY2000 Ultrace ICP Atomic Emission Spectrometer equipped with a JY AS 421 autosampler and 2400g/mm holographic grating. For ICP analysis, an aliquot of the NPs in hexane was dried and subsequently dissolved in warm (~75°C) aqua regia for 30 min to ensure complete dissolution of metal into the acid. The solution was then diluted with 2% HNO_3 solution for analysis.

NP Preparation for Electrocatalytic Evaluation.

The NPs were supported onto Ketjen carbon in a 1:2 wt. ratio. An appropriate amount of the Ketjen Carbon was measured and sonicated (Fischer Scientific FS 110) in a 20 mL of hexane and 5 mL of acetone for 30 minutes. Then, an appropriate wt. amount of NPs dispersed in 20 mL of hexane was added dropwise to the Ketjen carbon solution and kept for 1 h under sonication. The C-NP was recovered by centrifuging the mixture at 8000 rpm for 8 min. The colorless supernatant was discarded and the C-NP product was washed with hexane and dried under nitrogen. The C-NPs were annealed in air at 165 °C overnight. An appropriate amount of product was weighed and dispersed in deionized water, isopropanol, and Nafion in a 4:1: 0.025 to yield a suspension of 4 mg/mL C-NPs. All C-NP catalysts were prepared in the same manner.

Electrochemical Evaluation of NPs/C for FAOR

5μL of the 4 mg/mL C-NP suspension prepared above was dropped onto a rotating disk electrode (RDE) with a glassy carbon surface (5 mm in diameter). The electrochemical measurements were performed on an Autolab Potentiostat from Metrohm Instrument Company (Autolab 302) by a cyclic voltammetry technique. Ag/AgCl and a Pt mesh wire were used as the reference and counter electrodes, respectively. The NP catalysts were evaluated for the FAOR in nitrogen saturated 0.1 M $HClO_4$ + 0.2 M HCOOH solution at 25°C. The C-NP was first electrochemically cleaned by scanning the potential from -0.2 V to 0.9 V for 30 cycles at 100 mV/s. All subsequent measurements were then scanned at a rate of 50 mV/s. The mass current was normalized to mA/cm^2 by dividing the measured electrode currents over the electrochemically active surface area of the C-NP catalyst.

Supplemental Figures

Figure S1 – TEM image of the as-synthesized Pd NPs

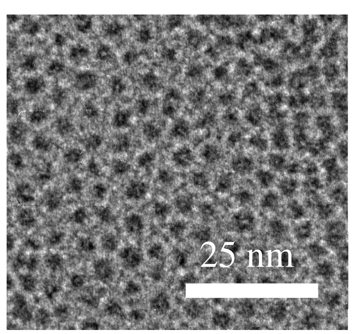

Figure S-2 : TEM images of the CoPd NPs synthesized at (A) 75 °C and (B) 125 °C

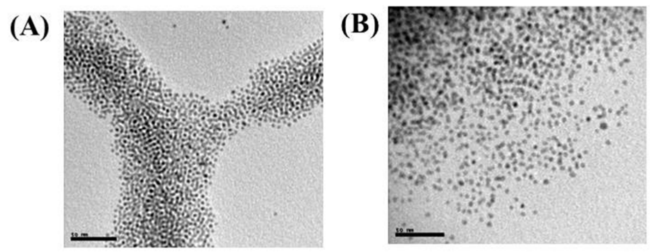

Figure S-3 : TEM image of the annealed C-CoPd catalysts